Received: 26 April 2022 | Revised: 27 October 2022 | Accepted: 9 December 2022

DOI: 10.1002/jbt.23280

RESEARCH ARTICLE

WILEY

Inhibition of autophagy reduces the rate of fluoride-induced LS8 apoptosis via regulating ATG5 and ATG7

Lin Zhao[1] | Han Wang[1] | Sijia Liu[1] | Tao Xi[1] | Liyuan Wang[1,2] | Yang Li[1] | Lu Chen[3] | Ruan Jianping[3] | Kristina Xiao Liang[4,5]

[1]Ningxia Key Laboratory of Cranio-maxillofacial Deformities, College of Stomatology, Ningxia Medical University, Yinchuan, China

[2]Stomatological Hospital of the General Hospital of Ningxia Medical University, Yinchuan, China

[3]Department of Preventive Dentistry, Clinical Research Center of Shaanxi Province for Dental and Maxillofacial Diseases, Stomatology Hospital, Xi'an Jiaotong University, Xi'an, China

[4]Neuro-SysMed, Center of Excellence for Clinical Research in Neurological Diseases, Department of Neurology, Haukeland University Hospital, Bergen, Norway

[5]Department of Clinical Medicine, University of Bergen, Bergen, Norway

Correspondence

Ruan Jianping, Department of Preventive Dentistry, Stomatology Hospital, Xi'an Jiaotong University, 98# Xiwu Rd, Xi'an 710004, Shaanxi, China.
Email: ruanjp@xjtu.edu.cn

Kristina Xiao Liang, Department of Clinical Medicine, University of Bergen, PO Box 7804, 5020 Bergen, Norway.
Email: xiao.liang@uib.no

Funding information

the National Natural Science Foundation of China, Grant/Award Number: 81860564; the First-Class Discipline Construction Found Project of Ningxia Medical University and the School of Clinical Medicine, Grant/Award Number: NXYLXK2017A05; the Natural Science Foundation of Ningxia, Grant/Award Number: 2018AAC03065

Abstract

Excessive fluoride affects ameloblast differentiation and tooth development. The fate of fluorinated ameloblasts is determined by multiple signaling pathways in response to a range of stimuli. Both autophagy and apoptosis are involved in the regulation of dental fluorosis as well as in protein synthesis and enamel mineralization. Emerging evidence suggests that autophagy and apoptosis are interconnected and that their interaction greatly influences cell death. However, the effect of autophagy on apoptosis in fluoride-treated ameloblasts is unclear. Here, we employed an in vitro cellular model of fluorosis in mouse ameloblast-like LS8 cells and induced autophagy using sodium fluoride (NaF). Our findings suggest that NaF treatment induces autophagy in LS8 cells, and ATG5 and ATG7 are important molecules involved in this process. We also showed that NaF treatment reduced cell viability in Atg5/7 siRNA and autophagy inhibitor-treated LS8 cells. More importantly, NaF-induced apoptosis can be reversed by inhibiting early stage of autophagy. In conclusion, our study shows that autophagy is closely related to dental fluorosis, and inhibition of autophagy, especially ATG5/7, reduces fluoride-induced cell death and apoptosis.

KEYWORDS

Apoptosis, autophagy, LS8, NaF

Lin Zhao and Han Wang contributed equally to this work.

1 | INTRODUCTION

Autophagy is a catabolic-driven process in which stressed cells form cytoplasmic, bilayer, crescent-shaped membranes called phagocytes, which mature into intact autophagosomes.[1–3] Autophagosomes engulf long-lived proteins and damaged cytoplasmic organelles to provide components for cellular energy production.[1–3] Studies have shown that autophagy is involved in the regulation of dental fluorosis, protein synthesis, and enamel mineralization.[4]

Our previous study confirmed that fluoride can induce apoptosis in LS8 cells.[5,6] The link between apoptosis and autophagy is complex. In some cases, autophagy is considered as a cell rescue strategy to prevent apoptosis.[7] Conversely, when apoptosis is inefficient, autophagy may promote apoptosis or alternative mechanisms that ultimately lead to cell death.[3,8,9] Autophagy is a cytoprotective mechanism that facilitates stress adaptation and prevents cell death. It has been demonstrated that autophagy and apoptosis usually occur in the same cell, and autophagy usually precedes apoptosis.[10] Furthermore, components of the autophagy and apoptotic pathways can interact with apoptosis within cells. Generally, autophagy blocks the induction of apoptosis by inactivating caspases, whereas apoptosis-associated caspase activation terminates the autophagy process by cleaving autophagy proteins. However, under specific conditions, autophagy or autophagy-related proteins may promote the induction of apoptosis and constitute an apoptotic alternative pathway leading to cell death (i.e., autophagic cell death).[11] However, few reports describe the relationship between autophagy and fluoride-induced apoptosis.

The fate of fluoride-treated LS8 cells is determined by multiple signaling pathways in response to a range of stimuli. Fluoride as an extracellular stimulus induces apoptosis in LS8 cells through endogenous, exogenous, and endoplasmic reticulum (ER) pathways.[5] Recent studies have shown that autophagy can induce apoptosis.[11] The interaction between 'self-feeding' (autophagy) and 'self-killing' (apoptosis) in fluoride-treated LS8 cells and the crosstalk between components are not well understood.[11,12]

In the previous study, we applied an established in vitro fluorosis induction system to induce fluorosis using murine ameloblast-like LS8 cells and sodium fluoride (NaF).[5,6,13] In this study, we used this in vitro fluorosis-inducing system and investigated the effect of fluoride on LS8 cell-induced apoptosis by autophagy. We performed short interfering RNAs (siRNAs) against Atg5 and Atg7 to inhibit the expression of autophagy-related genes in LS8 cells and detected LS8 cell activity and apoptosis porpotion. Then, LS8 cells were infected with adenovirus carrying double-labeled autophagy-related mRFP-GFP-LC3, and then, the infected cells were transfected with Atg5/7 siRNAs. We detected LS8 cell activity, autophagy, and apoptosis. LS8 cells were pretreated with 3-methyladenine (3-MA), an early autophagy inhibitor, and bafilomycin-A1 (BAF-A1), a late autophagy inhibitor, to detect LS8 cell activity and apoptosis porpotion. Our results revealed that inhibition of autophagy can reduce the rate of fluoride-induced apoptosis LS8 cell death (supplement Figure 1A).

2 | MATERIALS AND METHODS

2.1 | Cell culture and treatments

The mouse ameloblast-like cell line (LS8 cell line) was cultured in Dulbecco's modified Eagle's medium supplemented with 10% fetal bovine serum, 100 units/ml penicillin, and 100 mg/ml streptomycin (Invitrogen). After reaching 70%–80% confluence, the cells were incubated with serum-free medium containing the indicated concentrations (2 mM) of NaF. After NaF treatment, the cells were incubated for 24 h or 48 h at 37°C.

2.2 | Chemicals and antibodies

Rabbit LC3 I/II (Cat# WL01506, RRID:AB_2910622), Beclin1 (Cat#WL02508, RRID:AB _2910618), p62 (Cat#WL02385, RRID:AB_2910619), caspase3/cleaved caspase3 (Cat# WL02117, RRID:AB_2910623), PARP/cleaved PARP (Cat#WL01932, RRID:AB_2910624), bcl-2(Cat#WL01556, RRID:AB_2904235) and β-actin (Cat#WL01845, RRID:AB_2910630) were purchased from Wanleibio. Calpain 1 was purchased from ABclonal Technology (Cat#A8710, RRID:AB_2863593), and caspase 12/cleaved caspase 12 was purchased from Abcam (Cat# ab62463, RRID:AB_955730). All antibodies were used at a dilution ratio of 1:500 ~ 1:2000 for western blot analysis. Anti-rabbit secondary antibodies were purchased from Wanleibio (Cat# WLA023, RRID:AB_2890057). The inhibitors 3-methyladenine (3-MA, Selleck) and bafilomycin-A1 (Baf-A1) were purchased from Cell Signaling Technology (Medchemexpress, HY-100558). All procedures were performed with approval from the Ethics Committee at Ningxia Medical University, Yinchuan, China.

2.3 | Protein extraction

LS8 cells were washed with chilled phosphate-buffered saline and lysed in ice-cold radioimmunoprecipitation assay buffer as previously described. Cell lysate was collected using a cell scraper (Corning), and the homogenate was sonicated on ice for 30 min. The lysate was collected by centrifugation at 12,000×*g* for 15 min at 4°C. The protein content was determined using a bicinchoninic assay (BCA) protein assay kit (Wanleibio) by extrapolation on the basis of dye binding in a standard series of known protein concentrations determined using spectrophotometry.

2.4 | Western blot analysis (WB)

Supernatants with an equal mass of protein for each experimental condition were mixed with loading buffer (5-sodium dodecyl sulfate, 5% v/v) and denatured by heating at 95°C for 5 min. Lysate proteins were resolved according to size in 10%–12% sodium dodecyl

sulfate-polyacrylamide gel electrophoresis (SDS-PAGE) gels and transferred to a 0.22-μm polyvinylidene fluoride (PVDF) membrane (Millipore) using a semidry blotting system (Bio–Rad). Nonspecific absorption of antibodies on the membrane was blocked by incubation with 5 g% (w/v) skim milk in Tris-buffered saline (with 0.05% (v/v) Tween-20 for 2 h. Samples were incubated overnight with one of the primary antibodies at 4°C. The membrane was washed three times with 0.1% Tween-20 TBS for 10 min each time and incubated with the appropriate horseradish peroxidase-conjugated anti-rabbit or anti-mouse secondary antibody (1:10,000) against each primary antibody for 1 h at room temperature. After washing with TBS-0.1% in Tween-20 three times, an enhanced chemiluminescence kit (Millipore) was used to detect immunoreactive protein bands. The blots were immunodetected with an anti-β-actin antibody (1:1000) to confirm that proteins were loaded at an equal mass. The intensity of each immunoreactive protein band was quantified using a Quantity One densitometer (Bio–Rad).

2.5 | Transient transfection of short interfering RNAs (siRNAs)

LS8 cells were cultured in a 6-well plate, and upon reaching 40% confluence, the LS8 cells were transfected with siRNAs that had been synthesized by Jtsbio-tech (Jtsbio) against Atg5 and Atg7. The siRNAs were transfected using 7.5 μl of Lipofectamine 3000 (Invitrogen) according to the manufacturer's protocol. The cells were cultured in an incubator at 37°C with 5% CO_2. The cells were analyzed after 2.0 mmol/L NaF treatment for 24 and 48 h.

2.6 | RNA extraction and quantitative real-time polymerase chain reaction (qRT–PCR)

Total RNA was extracted from cells using TRIzol reagent (Carlsbad) according to the manufacturer's instructions. The quality and quantity of the isolated RNA was examined using a NanoDrop 2000/2000C spectrophotometer by measuring the absorbance at 260/280 nm. qRT–PCR was performed in a 20 μl volume of reaction mixture on an Applied Biosystems 7500 Real-Time PCR System (Thermo Fisher) with the following program: an initial denaturation of 5 min at 94°C, followed by 40 cycles of 94°C for 10 s, 60°C for 20 s, and 72°C for 30 s. Primers used in the amplification were designed and synthesized by GenScript (Nanjing). The sequences of the PCR primers were as follows: Atg5, F, 5′-AAGGATGCGGTTGAGGCT-3′, and R, 5′-GCTCCGTCGTGGTC TGAT-3′; Atg7, F, 5′-TGGGAGAAGAA CCAGAAAG-3′, and R, 5′-TCAGTGTCCTAGCC ACA TTAC-3′; and β-actin (the internal control), F, 5′-CTGTGCCC ATCTACGAGG GCTAT-3′, and R, 5′ TTTGATGTCACGCACGATTTCC-3′. A melting curve analysis was performed on each amplicon to ensure that a single PCR product was amplified. The relative expression levels were calculated using the comparative threshold cycle (△△CT) method.

2.7 | Analysis of cell viability

A Cell Counting Kit-8 (CCK-8) (Wanleibio, Wuhan, China, WLA074) assay was performed to measure cell viability. LS8 cells were cultured in a 96-well plate and exposed to various treatments for 24 and 48 h, according to the manufacturer's protocol. Each group was seeded with 4×10^3 cells, and each group was cultured in 5 duplicate wells. Then, the cells were incubated with 10 μl of CCK-8 reagent at 37°C for 2 h. The optical density (OD) values were read at 450 nm with a microplate reader (BIOTEK 800Ts). Cell viability is expressed in terms of the OD value.

2.8 | Analysis of the apoptosis porpotion

LS8 cells were seeded at 4×10^6 cells/ml in six-well plates. The cells were inoculated according to experimental groups and were treated with drugs or transfection after cell adherence. Cells were harvested by trypsinization, washed with cold PBS. The cells were resuspended in 300 μl of 1x binding buffer and transferred to a sterile flow cytometry (FCM) glass tube. Five microliters of Annexin V–fluorescein isothiocyanate (FITC) and 10 μl of propidium iodide (PI) was added, and the cells were incubated in the dark for 15 min at room temperature and analyzed with a flow cytometer (Eisen Biological). The number of apoptotic cells was determined using Annexin V–FITC Apoptosis Detection Kit I (Wanleibio, WLA001).

2.9 | Fluorescence microscopy

LS8 cells were seeded in six-well plates and incubated for 24 h, LS8 cells were exposed to various treatments for 24 and 48 h. Only medium was added to blank control group wells, and each group was established with one duplicate well. Then, the cells were washed once with ice-cold PBS, and 0.5 ml of Hoechst 33342 staining solution (Wanleibio, WLA042a) was added to each group for 20 min at 37℃ in the dark. After three washes with PBS, the stained nuclei and morphological changes of cells were observed through fluorescence microscopy.

2.10 | Confocal microscopy

LS8 cells were plated in 24-well plates and allowed to reach 50%–70% confluence before transfection. mRFP-GFP-LC3 adenoviral vectors were purchased from HanBio Technology. The principle of the assay is based on the different pH stabilities of the GFP and RFP. The fluorescence signal emitted by EGFP was quenched under acidic conditions (a pH <5) inside lysosomes, and the mRFP fluorescence signal showed no significant change under acidic conditions. In the merged green and red fluorescence images, autophagosomes are shown as yellow puncta (i.e., RFP + GFP +), while autolysosomes are shown as red puncta (i.e., RFP + GFP −).

Increased autophagic flux is indicated when the number of both yellow and red puncta are increased in cells, while inhibited autophagic flux is indicated when only the number of yellow puncta is increased but the number of red puncta remains unchanged or when the numbers of both yellow and red puncta are decreased in cells.[14]

Adenoviral infection was performed according to the virus manufacturer's instructions. LS8 cells were incubated in growth medium with adenovirus for 6 h at 37°C, the medium supernatant containing virus was discarded and replaced with complete medium, and the cells were incubated at 37°C with 5% CO_2 for 24 h. After 24 h, dosing or transfection was performed. LC3 puncta were examined with an Olympus confocal microscope (FV1000S-SIM/IX81).

2.11 | Statistical analysis

Statistical analyses were performed using SPSS software, Version 18.0 (SPSS Inc). All data are expressed as the means ± standard deviation (SD), and each experiment was performed in triplicate. Differences between groups were assessed for significance by one-way analysis of variance (ANOVA) or two-way ANOVA. When variances were uniform, the results of pair comparisons determined by least significant difference (LSD) *t*-tests are reported. When variances were not uniform, the results of pair comparisons determined by Dunnett T3 test and Games–Howell test are reported. For all analyses, two-tailed *p* values less than 0.05 were considered significant.

3 | RESULTS

3.1 | Fluoride-induced autophagy in LS8 cells

To examine the effect of fluoride on autophagy, we first treated the LC8 cells with a serial dilution of NaF: 1 mmol/L, 2 mmol/L and 4 mmol/L for 24 h or 48 h (Figure S1B). We then performed western blot analysis to identify autophagy-related proteins LC3, Beclin1 and p62 and compared their protein expression with untreated cells. We found that Beclin 1 expression was significantly increased after 24 h of treatment with 2 mmol/L and 4 mmol/L NaF compared with the control group (Figure 1A a&b). Beclin 1 expression was significantly increased in all concentration groups after 48 h of NaF treatment (Figure 1A a&c). After 24 and 48 h of NaF treatment, p62 protein expression levels were significantly lower in all concentration groups than in the control group (Figure 1A a, d, e). Similar to the results of Beclin 1, the LC3II/I ratio of the control group was significantly higher than that of the sodium control group after 24 h of fluoride treatment at 4 mmol/L and 2 mmol/L and 4 mmol/L for 48 h (Figure 1A a, f, g). These observations suggest that NaF induces autophagy with a dose-time-dependent manner in LS8 cells.

These findings suggest that NaF can induce autophagy in LS8 cells with a dose-time-dependent manner.

3.2 | Fluoride induces the autophagy via regulating ATG5 and ATG7

ATG5 and ATG7 are essential molecules for the induction of autophagy.[15] We then used short interfering RNAs (siRNAs) targeting Atg5 and Atg7 to inhibit the expression of autophagy-related genes in LS8 cells and examined the expressions of autophagy-related protein Beclin 1, P62 and LC3B using western blot analysis. In addition, we examined the cells with or without NaF or with NaF alone for 24 h and 48 h. We found that the expression of autophagy-related protein Beclin 1 in the cells with NaF alone was significantly higher than control cells, and it was the highest among all the other treated groups (Figure 1Da,b.e,f). We detected a significantly lower Beclin 1 expression in the cells with Atg5/7 siRNA than control cells ((Figure 1D a,b.e,f), whereases the expressions were elevated after NaF treatment (Figure 1D a,b.e,f). In addition, the ratio of LC3 II/LC3I showed the same changes as Beclin 1 expression (Figure 1D a,d.e,h). Meanwhile, the expression of autophagy-related protein p62 was opposite to that of Beclin 1 expression and LC3II/I ratio (Figure 1D a, c.e,g). These changes were all the same for 24 h and 48 h.

These findings suggest that fluoride treatment can lead to the autophagy and ATG5 and ATG7 are involved in this process.

3.3 | Fluoride reduces the cell viability in Atg5/7 siRNA and autophagy inhibitor-treated LS8 cells

Nest, we silenced the expression of autophagy-related genes Atg5 or Atg7 and then applied CCK-8 assay to investigate the changes in cell viability of fluoride-treated LS8 cells. We used siRNA for Atg5 or Atg7 to treat the LS8 cells with or without NaF or with NaF alone for 24 and 48 h. Compared to control cells, we detected a significant reduction in cell viability in NaF-treated cells compared to control cells, whereases the cells in the presence of siRNA Atg5+NaF and siRNA Atg7+NaF showed similar cell viabilities (Figure 1B). When comparing with the NaF-treated cells, we found significantly increased cell viability in the cells treated with Atg5 siRNA and Atg7 siRNA groups, which was also higher than all the other groups. After being treated with NaF, the cell viability in Atg5 siRNA and Atg7 siRNA groups was significantly decreased (Figure 1B).

We further applied the autophagy inhibitors to investigate the changes in the cell activity. We pretreated LS8 cells with the early autophagy inhibitor 3-MA (10 mM) and/or the late autophagy inhibitor Baf-A1 (20 nM) for 2 h, and then treated with 2 mmol/L NaF for 24 h or 48 h. We showed that pretreatment with 3-MA and/or Baf-A1 reversed the NaF-induced decrease in cell viability compared to the control cells and cells treated with NaF (Figure 1C).

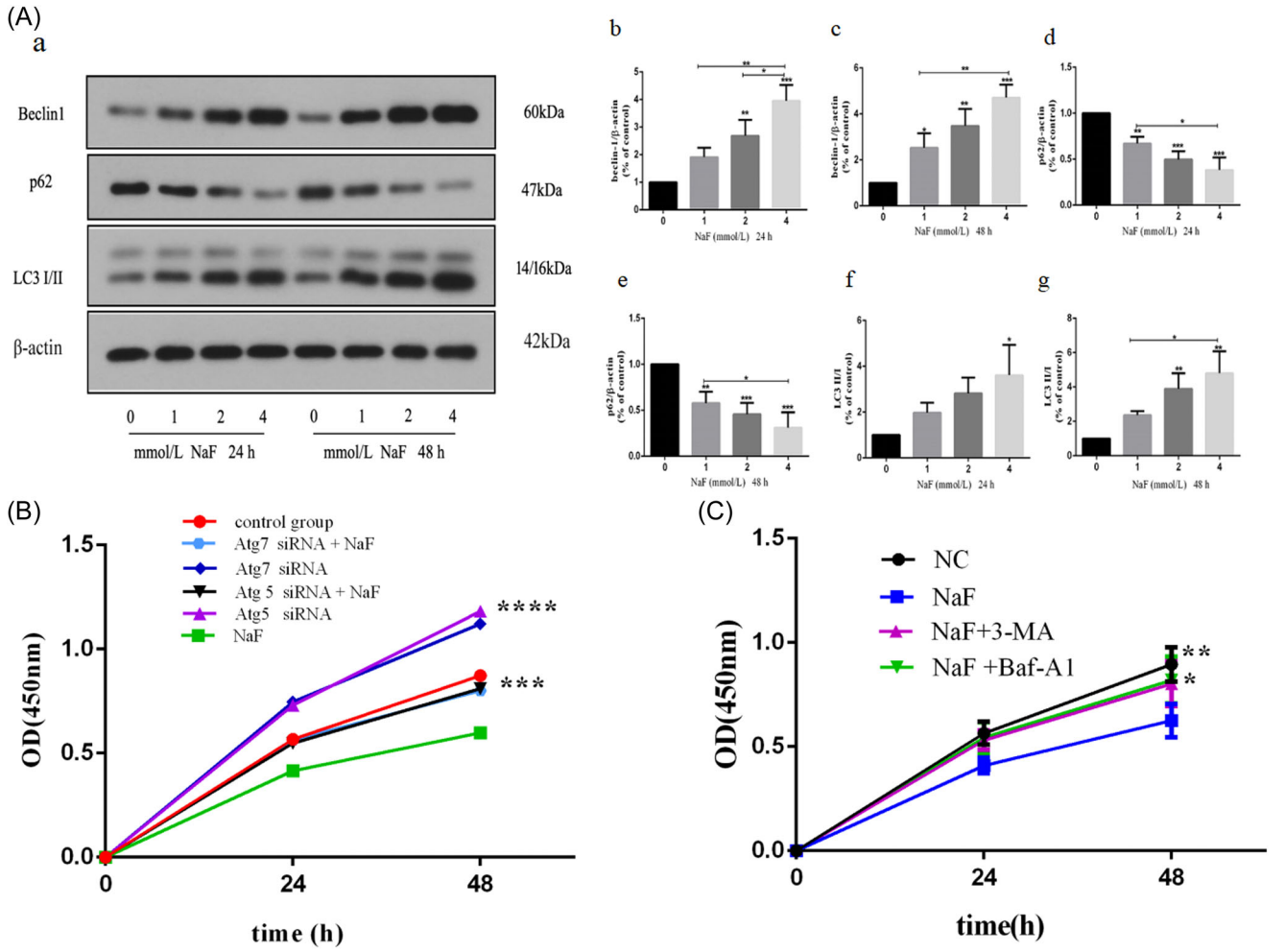

FIGURE 1 Western blot analysis the expression of autophagy-related proteins in LS8 cells treated with NaF for 24 h or 48 h. (A) LS8 cells treated with NaF at different concentrations (0, 1, 2, and 4 mmol/L). Cell viability was analyzed using Cell Counting Kit-8 (CCK-8). (B) Pretreatment with short interfering RNAs (siRNAs) against Atg5/7; (C) Pretreatment with 3-MA and Baf-A1. Error bars represent standard deviation (SD) based on triplicate experiments; the results are shown as the mean ± SD; $^{*}p < 0.05$& $^{**}p < 0.01$ (B,C with the control group* $p < 0.05$& $^{**}p < 0.01$).

These findings suggest that fluoride treatment reduces cell viability, which can be reversed by inhibiting autophagy.

3.4 | Fluoride induces the cell apoptosis, which is reversed by inhibiting the autophagy

We next performed FCM analysis using V-FITC/PI double staining to examine the rate of apoptosis in LS8 cells treated with Atg5/7 siRNA with or without NaF or with NaF alone for 24 h or 48 h. Compared with the control group, we found that NaF induced a significant increase in the pre and postapoptosis [(Q2 + Q4) %] (Figure 2A,B). The cells treated with Atg5/7 siRNA significantly reduced the number of apoptotic cells compared to NaF-treated LC8 cells (Figure 2A,B). At the same time, we found that the number of apoptotic cells in the Atg5/7 siRNA+NaF group was higher than that in the Atg5/7 siRNA group. The number of apoptotic LS8 cells was significantly reduced in the Atg5/7 siRNA + NaF group compared to the number of cells treated with NaF alone (Figure 2A,B). These changes were consistent between groups treated at 24 and 48 h (Figure 2A,B).

We also stained cells with Hoechst 33342 and then used fluorescence microscopy to observe the difference in cell morphology between the control and treatment groups. We found that the nuclei of LS8 cells in the control group were round light blue with dark blue granules and were uniformly stained, indicating that the nuclei had normal morphology and complete structure (Figure 2E). Then we observed the cells after NaF using the same method, we found that LS8 nuclei were lobulated, fragmented, and located near the cell membrane after treatment with 2 mmol/L NaF for 24 h and 48 h, and at the same time apoptotic cells appeared as evidence by the nuclei of the cells showing bright blue due to the DNA concentration (Figure 2E). In addition, NaF-treated cells were oblate, the nuclear envelope disappeared, chromatin was reduced, and the

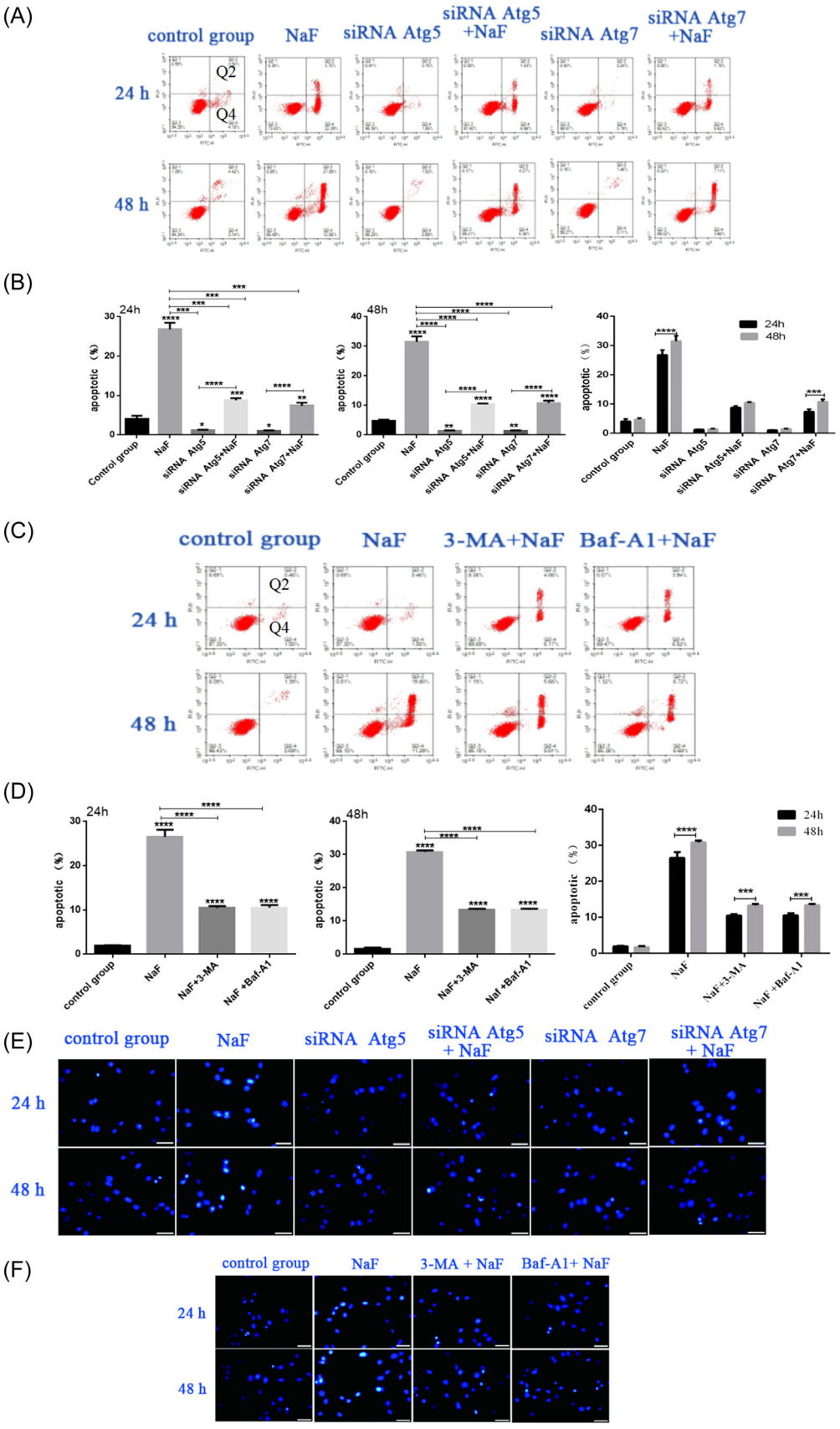

FIGURE 2 (See caption on next page)

nucleus was fragmented (Figure 2E). We observed that some nuclei were "crescent shaped" or "petal shaped" (Figure 2E). Meanwhile, the morphological changes were more obvious with the increase of NaF exposure (Figure 2E). Bright blue or lobulated stained nuclei appeared close to the cell membrane of apoptotic cells. After quantification, we found that the number of bright blue apoptotic cells was the highest in the NaF group, followed by the Atg5/7 siRNA + NaF group, and a small number of apoptotic cells were observed in the Atg5/7 siRNA group and the control group (Figure 2E).

Next, we treated LS8 cells with autophagy inhibitors to observe their effect on NaF-induced apoptosis. We again performed FCM analysis using Annexin V-FITC/PI double staining to detect 2 h treatment with the early autophagy inhibitor 3-MA and/or the late autophagy inhibitor Baf-A1 and NaF alone for 24 h and 48 h. Changes in apoptosis. We found that NaF treatment significantly increased the rate of apoptosis [(Q2 + Q4) %] (Figure 2C,D). The number of LS8 cells undergoing NaF-induced apoptosis was significantly reduced after pretreatment with autophagy inhibitors 3-MA and Baf-A1 (Figure 2C,D). The similar changes were detected in the cells treated for 24 h and 48 h (Figure 2C,D).

We again stained with Hoechst 33342 and observed LS8 cell morphology and nuclei under a fluorescence microscope. We found the highest number of bright, blue-stained apoptotic cells in the NaF group (Figure 2F). The number of apoptotic cells-stained bright blue with Hoechst 33342 was significantly reduced after pretreatment with the autophagy inhibitor 3-MA and/or Baf-A1 (Figure 2F).

These findings suggest that NaF treatment induces cell apoptosis, which can be reversed by inhibiting autophagy.

3.5 | Fluoride treatment leads to the cell apoptosis in LS8 cells, which can be reversed by inhibition of autophagy

We next examined the expression of apoptosis-related proteins in cells pretreated with Atg5/7 siRNA with or without NaF or with NaF alone for 24 and 48 h using western blot analysis. We found that the expression level of apoptotic key protein cleaved caspase3 in NaF group was significantly higher than that in other experimental groups (Figure 4A, a&f). After Atg5/7 siRNA pretreatment and the addition of NaF, the expression levels of cleaved caspase-3/caspase-3 were increased compared to those treated with Atg5/7 siRNA alone but decreased compared with the NaF treatment group (Figure 4A a&f). The expression trends of apoptotic proteins cleaved caspase12/caspase12, cleaved PARP/PARP, and Calpain1 were similar to those of cleaved caspase3/caspase3 (Figure 4A b-d). The expression of the antiapoptotic protein Bcl-2 showed an opposite trend to that of cleaved caspase-3/caspase-3 (Figure 4A e). These changes were the same for 24 h and 48 h (Figure 4B a-f). The expression of Beclin I in the NaF group was significantly higher than that in the control group (Figure 3A, a&b). After pretreatment of Atg5/7 siRNA followed by NaF treatment, we found a significant decreased level of Beclin I expression compared with that in cells treated with NaF alone (Figure 3A a&b). The ratio of LC3II/I ratio showed a same trend as that of the Beclin I expression (Figure 3A a&d), while the p62 showed the opposite changes than those of Becline 1 and LC3 (Figure 3A a&c). No differences were noticed in the cells treated with 24 h and 48 h (Figure 3B a–d).

Next, we measured the apoptosis proportion of LS8 cells treated with the early autophagy inhibitor 3-MA and/or the late autophagy inhibitor Baf-A1 for 2 h with or without NaF and those treated with only NaF for 24 h or 48 h. Western blot analysis showed that the expression level of the key apoptosis protein cleaved caspase3 in the NaF group was significantly higher than it was in other experiment groups (Figure 4C a&f). Pretreatment with autophagy inhibitors reduced the apoptosis of NaF-treated cells. The expression of the apoptotic proteins cleaved caspase-12/caspase-12, cleaved PARP/PARP and Calpain1 showed a similar trend to that of cleaved caspase-3/caspase-3 (Figure 4C a&b-d). The expression of the antiapoptotic protein Bcl-2 showed the opposite trend of cleaved caspase3/caspase3 (Figure 4C a&f). The expression of Beclin I in the NaF group was significantly higher than that in the control group (Figure 3C a&b). After pretreatment of early autophagy inhibitors 3-MA followed by NaF treatment, we found a significant decreased level of Beclin I expression compared with that in cells treated with NaF alone (Figure 3C a&b). Conversely, pretreatment of the late autophagy inhibitors Baf-A1 in NaF-treated cells showed an increased level of Beclin I expression in compared with the cells in the present of NaF alone (Figure 3C a&b). The ratio of LC3II/I ratio showed a same trend as that of the Beclin I expression (Figure 3C a&d), while the p62 showed the opposite changes than those of Becline 1 and LC3 (Figure 3C a&c). No differences were noticed in the cells treated with 24 h and 48 h (Figure 3C e–g).

This evidence suggests that fluoride treatment can induce apoptosis, which can be reversed by inhibiting the early stages of autophagy.

FIGURE 2 Apoptosis of LS8 cells were treated with siRNA Atg5/7 and autophagy inhibitor(s) and/or with NaF for 24 h or 48 h. The apoptosis porpotions were determined by flow cytometry (FCM) analysis of Annexin V–FITC/PI dual staining. Q1 quadrant (Annexin V, PI +) represents dead cells; Q2 quadrant (Annexin V + , PI +) represents late apoptotic cells; Q3 quadrant (Annexin V, PI) represents live cells; and Q4 quadrant (Annexin V + , PI) represents early apoptotic cells. (A-B) Pretreatment with siRNA5 and siRNA7;(C-D) Pretreatment with 3-MA and Baf-A1. Fluorescence microscopy was performed to observe the number of apoptotic cells stained bright blue with Hoechst 33342. (E) Pretreatment with siRNA Atg5/7; (F)Pretreatment with 3-MA and Baf-A1. Morphological changes in apoptotic cells revealed by Hoechst 33342 staining were observed with fluorescence microscopy. Scale bar = 10 μm. PI, propidium iodide; siRNA, small interfering RNA.

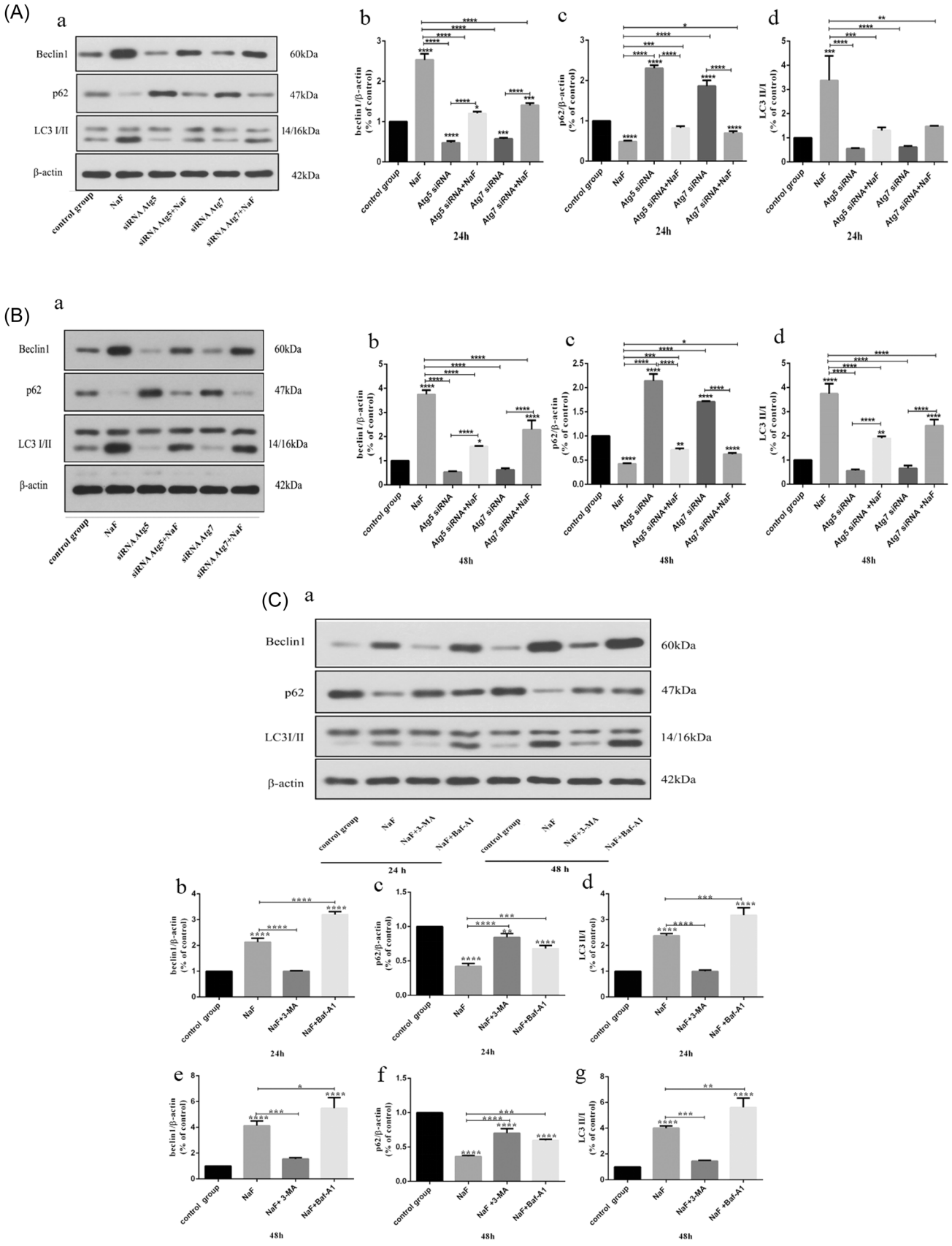

FIGURE 3 Western blot analysis the expression of autophagy-related proteins in LS8 cells treated with NaF for 24 h or 48 h were detected after pretreatment with siRNA Atg5/7 and 3-MA/Baf-A1. (A and B) Pretreatment with siRNA Atg5/7 24 h; (C and D) Pretreatment with siRNA Atg5/7 48 h; (E and F) Pretreatment with 3-MA and Baf-A1 for 24 h or 48 h. siRNA, small interfering RNA.

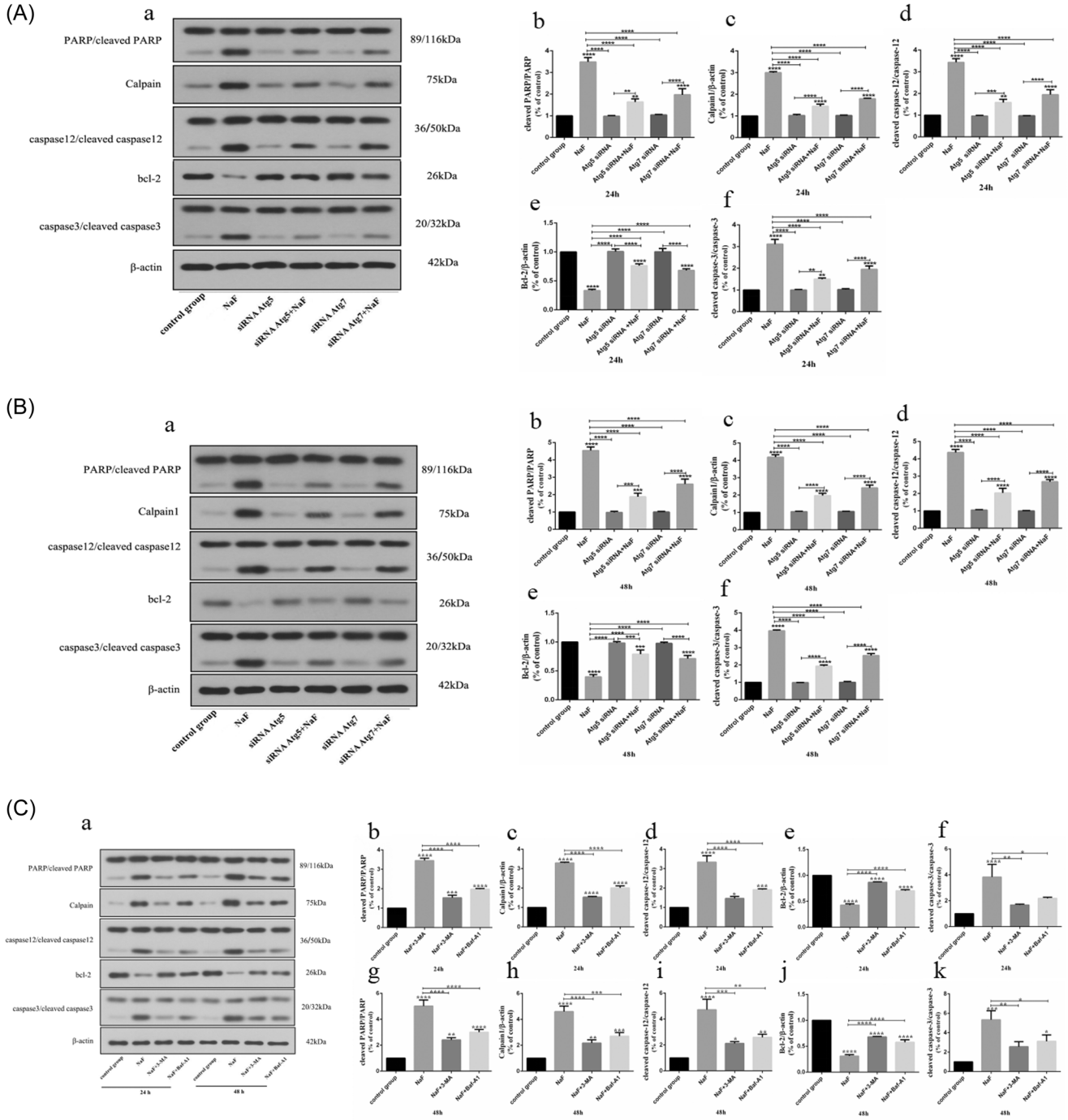

FIGURE 4 Western blot analysis the expression of apoptosis-related proteins in LS8 cells treated with NaF for 24 h or 48 h were detected after with 3-MA and Baf-1 pretreatment. (A and B) Pretreatment with siRNA Atg5/7 24 h; (C and D) Pretreatment with siRNA Atg5/7 48 h; (E and F) Pretreatment with 3-MA and Baf-A1 for 24 h or 48 h. siRNA, small interfering RNA.

3.6 | Fluoride treatment can lead to the autophagy flux through mediation of ATG5 and ATG7 signaling

Given monitoring autophagic flux is important for the analysis of autophagy, we further examined the autophagic flux to confirm the findings described above. we first infected the LC8 cells with adenovirus carrying double-tagged autophagy-related mRFP-GFP-LC3, and then transfected the mRFP-GFP-LC3 labeled cells with Atg5/7 siRNA. After cell transfection, cells with green fluorescent (GFP) signal indicated autophagolysosome formation, and cells showed red fluorescence indicating LC3 staining. Due to the acid sensitivity of GFP fluorescent protein, when autophagosomes fuse with lysosomes, GFP fluorescence is quenched, and only red fluorescence is detected. All the red spots represent autophagolysosomes, and the yellow spots that appear after fusion of red and green, fluorescent images represent autophagosomes. Confocal

microcopy analysis demonstrated an increased number of autophagosomes in NaF treated cells than controls (supplemental Figure 2A,B). After treatment with Atg5/7 siRNA, the number of autophagosomes in the LS8 cells decreased (Figure S2A). After intervention with NaF, the number of autophagosomes in the LS8 cells increased compared with that in the Atg5/7 siRNA group and decreased compared with that in the NaF-only treatment group (Figure S2A). These changes were slightly different at 24 h and 48 h (Figure S2B). Again, we treated LS8 cells with early autophagy inhibitor 3-MA and late autophagy inhibitor Baf-A1 and found that NaF exposure increased amount of autophagy in LS8 cells (Figure S2C,D). The 3-MA treatment reduced the numbers of autophagosomes in NaF treated cells compared the untreated cells (Figure S2C). We found decreased autophagolysosome formation in LS8 cells pretreated with Baf-A1 (Figure S2C). The above changes were more pronounced at 48 h than at 24 h (Figure S2D).

These evidence confirm the findings demonstrated above, which is that fluoride treatment can lead to the autophagy flux through mediation of ATG5 and ATG7 signaling.

4 | DISCUSSION

4.1 | NaF induces autophagy in LS8 cells

Autophagy is a lysosomal catabolic pathway that recycles damaged cytosolic macromolecules and organelles under cellular stress and exerts survival-promoting and death-promoting effects that are dependent on various stresses. For example, in stem/progenitor cells, autophagy mitigates metal-induced toxicity and contributes to the maintenance of tissue renewal capability.[16]

Studies have shown that, compared to stratified nonsecretory epithelial cells, epithelial cells (e.g., ameloblasts) in secretory organs show a greater need to undergo autophagic flux to maintain homeostasis.[2] A study indicated that autophagy is required for normal murine tooth biology.[2] In our study, we found that in LS8 cells, fluoride increased the level of LC3 II, which is an indicator of autophagosome formation. The LC3-I-to-LC3-II conversion was notably increased in the western blot analysis, verifying that autophagy was induced by fluoride.

In the early stage of autophagy, LC3 and Beclin 1 are required for autophagosome formation. Our study showed that fluorinated LS8 cells not only showed increased expression of LC3 but also increased expression of Beclin1, following the same trend. Conjugation of phosphatidylethanolamine to the C-terminus of LC3-I leads to the LC3-II form, which is an indicator of autophagosomal membrane formation. Beclin 1 is part of a multiprotein interactome that controls the initiation of autophagy and thus plays a critical role in cellular housekeeping and homeostatic maintenance.[17,18]

Additionally, p62, an important LC3-interacting protein upon autophagy stimulation, is normally degraded during autophagy and accumulates when autophagy is impaired.[19] In the present study, NaF treatment increased the expression of autophagy-related proteins in LS8 cells, including Beclin-1 and LC3-II, and induced autophagic flux, as evidenced by p62 degradation, in LS8 cells.

For determination of the effect of fluoride treatment on autophagy in LS8 cells, LS8 cells were pre-exposed to 3-MA and Baf-A1 and then treated with fluoride. The early autophagy inhibitor 3-MA inhibits autophagosome formation by inhibiting Class III PI3K. Baf-A1, a late autophagy inhibitor, can acidify H^+ -ATPase proton pump inhibitors of vesicle substances in autophagy, and H^+ -ATPase is the key enzyme for lysosomal development and maturation. Baf-A1 inhibits vesicle acidification and then inhibits autophagosome formation. The results showed that 3-MA treatment decreased the LC3-II/LC3-I ratio in LS8 cells that had been induced by fluoride and inhibited the transformation from LC3-I to LC3-II. In contrast, the effect of Baf-A1 was similar to that of fluoride. The synergistic effect of the two inhibitors led to an increase in the LC3-II/LC3-I ratio in LS8 cells, and the transformation from LC3-I to LC3-II was accelerated, which was more obvious than the effect of NaF treatment alone. These data suggest that 3-MA interferes with or blocks fluoride-induced autophagosome formation in LS8 cells, whereas Baf-A1 activates fluoride-induced autophagic lysosomes in LS8 cells.

4.2 | Inhibition of autophagy can reduce the rate of fluoride-induced apoptosis LS8 cell death

Autophagy can lead to autophagic cell death,[20] and autophagy has been found to facilitate induce apoptosis by activating apoptosis-related proteins.[21] Autophagy also can promote cell proliferation and cell survival in an attempt to cope with stress and prevent cell apoptosis.[22] In this study, we found that the NaF-induced LS8 cell apoptosis proportion was reduced and that the proliferative activity of LS8 cells was increased after autophagy-related genes were silenced. Then, we treated LS8 cells with both an early and late autophagy inhibitor and found the same results. These findings suggested that fluoride-induced autophagy in LS8 cells and that excessive autophagy resulted in the apoptosis of LS8 cells due to the high concentration of fluoride. Therefore, when LS8 cell autophagy was inhibited in the experimental process, the apoptosis proportion of LS8 cells was reduced.

Autophagy compounds extensively communicates with apoptosis compounds to determine cell fate under a myriad of physiological and pathological conditions.[23,24] Autophagy and apoptosis are two evolutionarily conserved processes that play crucial roles in determining cell fate. Despite the marked differences between these two catabolic processes, autophagy and apoptosis are intimately connected with each other. In the majority of cases, autophagy and apoptosis tend to be mutually inhibitory. To observe the relationship between autophagy and apoptosis in LS8 cells treated with fluoride, we used a variety of methods to observe apoptosis after inhibiting autophagy activity. First, we silenced the Atg5 and Atg7 genes in LS8 cells and observed the activity and apoptosis of these LS8 cells after fluoride treatment. The results showed that the absence of the Atg5

or Atg7 genes inhibited the autophagic activation in fluoride-treated LS8 cells, and silencing Atg5/7 in cells protected LS8 cells from fluoride-induced apoptosis. We also found that the activity of LS8 cells increased after the Atg5 and Atg7 genes were silenced. These results indicated that we can inhibit autophagy by silencing the expression of autophagy-related genes, resulting in a lower apoptosis porpotion and increased cell activity. Studies have shown that inactivation of either Atg5 or Atg7 disrupts autophagic flux, and global knockout of the Atg5 or Atg7 genes in mice results in perinatal lethality.[25] Despite the progress made in understanding the contribution of autophagy to tissue homeostasis, the physiological functions of autophagy in many cell types, such as ameloblasts, remains elusive.

Several mechanisms underlie the interaction of apoptosis and autophagy pathway components.[26,27] Studies have shown that inhibition of autophagy can promote oxidative injury and DNA damage and increase subsequent activity of caspase-3 and PARP1, which are involved in the apoptosis.[28] In our study, we found that the activity of caspase-3, caspase-12, calpain and PARP1 in LS8 cells after NaF treatment was decreased compared with that in LS8 cells treated only with NaF after autophagy-related genes were silenced or early and late autophagy inhibitors were applied. The mechanism of autophagy inducing changes in apoptosis-related proteins remains to be further explored. We also found that the trend of Bcl-2 expression was the opposite that of the aforementioned proteins. This study confirmed that inhibition of autophagy by fluoride in LS8 cells inhibited apoptosis. Studies have shown that the dissociation of Beclin1 from Bcl-2 is essential for autophagy and that Bcl-2 inhibits only autophagy when it is present in the ER. Beclin 1 complexes are involved in the early steps of autophagocytosis and endocytosis but not in the later phases of cargo transport to autolysosomes. The specific mechanism by which Beclin and Bcl-2 activity in LS8 cells is affected by fluoride treatment remains to be further studied.

In human endothelial cells undergoing apoptosis in conditions of nutrient shortage, activated caspase-3 favors the extracellular export of autophagic vacuoles by rerouting them toward the cell membrane.[29] The externalization of large autophagic vacuoles may contribute to the apoptosis-related decrease in cell size, a geometric determinant of cell disintegration into apoptotic bodies.[30] This evidence suggests that caspase-3 is a potential molecular switch in mediating crosstalk between autophagic and apoptotic program components.[29] In this study, the activity of caspase-3 and caspase-12 decreased after Atg5/7 were silenced. Previous studies have shown that the ER pathway (caspase-12) is involved in the apoptosis of LS8 cells under the action of fluoride. Caspases play a cardinal role in apoptotic cell death and a critical role in directing autophagy–apoptosis crosstalk. Processed caspases can shut off the autophagic response by inducing Atg protein (i.e., Beclin-1, Atg5, and Atg7) degradation.

In previous studies, we found that 3-Ma and Baf-A1 played different roles in autophagy activation in fluoridated LS8 cells, but their effects on apoptosis were consistent. These studies suggested that the autophagy induced in LS8 cells by 2 mM NaF treatment is critical to cell apoptosis. It is possible that autophagy can reduce the cell apoptosis porpotion of LS8 cells in the presence of low NaF concentrations. This possibility needs to be further studied. Increasing evidence has confirmed that apoptosis and autophagy are not independent pathways. There is a cooperative relationship between components of apoptosis and autophagy, which are two important catabolic processes with complex and intersecting protein networks contributing to the maintenance of cellular homeostasis.[31] Apoptosis may be initiated by autophagy, and autophagy may end with apoptosis.[32]

In this study, we found that inhibition of autophagy alleviates fluorine-induced apoptosis of LS8 cells. We believe that excessive autophagy caused by the concentration-dependent effects of NaF in this study leads to cytotoxicity not cell homeostasis and promotes cell survival. In some cases, inhibition of autophagy-related gene expression can reduce caspase shearing and apoptotic cell death. On the other hand, autophagy inhibitors can affect the apoptotic cascade by regulating the number and activity of caspase. Undoubtedly, these key findings add to our understanding of the unique role of caspase in autophagy - apoptotic transformation.

AUTHOR CONTRIBUTIONS

Lin Zhao, Han Wang, Tao Xi, Sijia Liu, Liyuan Wang, Yang Li, and Lu Chen contributed to the experimental investigation; Lin Zhao and Kristina Xiao Liang contributed to the writing of the original draft; all the authors contributed to reviewing and editing the manuscript, and Ruan Jianping and Kristina Xiao Liang contributed the resources and supervised the project. All authors read and approved the final manuscript.

ACKNOWLEDGMENTS

We thank Professor Malcolm L. Snead (Department of Biomedical Sciences, University of Southern California) for the donation of LS8 cells. This project was supported by grants from the National Natural Science Foundation of China (81860564), the Natural Science Foundation of Ningxia (2018AAC03065), the First-Class Discipline Construction Found Project of Ningxia Medical University and the School of Clinical Medicine (NXYLXK2017A05).

CONFLICTS OF INTEREST

The authors declare no conflicts of interest.

DATA AVAILABILITY STATEMENT

Data is openly available in a public repository that issues data sets with DOIs.

ORCID

Ruan Jianping http://orcid.org/0000-0002-7265-4375

REFERENCES

[1] S. Mukhopadhyay, P. K. Panda, N. Sinha, D. N. Das, S. K. Bhutia, *Apoptosis* **2014**, *19*(4), 555.

[2] S. Sukseree, U. Y. Schwarze, R. Gruber, F. Gruber, M. Quiles Del Rey, J. D. Mancias, J. D. Bartlett, E. Tschachler, L. Eckhart, *Autophagy* **2020**, *16*(10), 1851.
[3] M. S. D'Arcy, *Cell Biol. Int.* **2019**, *43*(6), 582.
[4] M. Suzuki, J. D. Bartlett, *Biochim. Biophys. Acta (BBA) - Mol. Basis of Dis.* **2014**, *1842*(2), 245.
[5] L. Zhao, J. Li, J. Su, M. L. Snead, J. Ruan, *Acta Odontol. Scand.* **2016**, *74*(7), 539.
[6] J. Li, L. Zhao, X. Zhao, P. Wang, Y. Liu, J. Ruan, *Biol. Trace Elem. Res.* **2018**, *181*(1), 104.
[7] R. Ojha, M. Ishaq, S. Singh, *J. Cancer Res. Ther.* **2015**, *11*(3), 514.
[8] A. Eisenberg-Lerner, S. Bialik, H. U. Simon, A. Kimchi, *Cell Death Differ.* **2009**, *16*(7), 966.
[9] P. Tsapras, I. P. Nezis, *Cell Death Differ.* **2017**, *24*(8), 1369.
[10] E. Wirawan, T. V. Berghe, S. Lippens, P. Agostinis, P. Vandenabeele, *Cell Res.* **2012**, *22*(1), 43.
[11] W. D. Fairlie, S. Tran, E. F. Lee, *Int. Rev. Cell. Mol. Biol.* **2020**, *352*, 115.
[12] M. C. Maiuri, E. Zalckvar, A. Kimchi, G. Kroemer, *Nat. Rev. Mol. Cell Biol.* **2007**, *8*(9), 741.
[13] L. Zhao, J. Su, S. Liu, Y. Li, T. Xi, J. Ruan, K. X. Liang, R. Huang, *Biochem. Biophys. Res. Commun.* **2021**, *542*, 65.
[14] C. Zhou, W. Zhong, J. Zhou, F. Sheng, Z. Fang, Y. Wei, Y. Chen, X. Deng, B. Xia, J. Lin, *Autophagy* **2012**, *8*(8), 1215.
[15] B. Levine, G. Kroemer, *Cell* **2019**, *176*(1-2), 11.
[16] M. Di Gioacchino, C. Petrarca, A. Perrone, S. Martino, D. L. Esposito, L. V. Lotti, R. Mariani-Costantini, *Autophagy* **2008**, *4*(4), 537.
[17] S. B. Thoresen, N. M. Pedersen, K. Liestøl, H. Stenmark, *Exp. Cell Res.* **2010**, *316*(20), 3368.
[18] C. Gordy, Y. W. He, *Protein Cell* **2012**, *3*(1), 17.
[19] Q. Zhang, X. Wang, S. Cao, Y. Sun, X. He, B. Jiang, Y. Yu, J. Duan, F. Qiu, N. Kang, *Biomed. Pharmacother.* **2020**, *128*, 110245.
[20] D. Denton, S. Nicolson, S. Kumar, *Cell Death Differ.* **2012**, *19*(1), 87.
[21] S. Song, J. Tan, Y. Miao, M. Li, Q. Zhang, *J. Cell. Physiol.* **2017**, *232*(11), 2977.
[22] P. Boya, R. A. González-Polo, N. Casares, J. L. Perfettini, P. Dessen, N. Larochette, D. Métivier, D. Meley, S. Souquere, T. Yoshimori, G. Pierron, P. Codogno, G. Kroemer, *Mol. Cell. Biol.* **2005**, *25*(3), 1025.
[23] L. Moretti, Y. I. Cha, K. J. Niermann, B. Lu, *Cell Cycle* **2007**, *6*(7), 793.
[24] G. Mariño, M. Niso-Santano, E. H. Baehrecke, G. Kroemer, *Nat. Rev. Mol. Cell Biol.* **2014**, *15*(2), 81.
[25] M. Komatsu, S. Waguri, T. Ueno, J. Iwata, S. Murata, I. Tanida, J. Ezaki, N. Mizushima, Y. Ohsumi, Y. Uchiyama, E. Kominami, K. Tanaka, T. Chiba, *J. Cell Biol.* **2005**, *169*(3), 425.
[26] S. Pattingre, C. Bauvy, S. Carpentier, T. Levade, B. Levine, P. Codogno, *J. Biol. Chem.* **2009**, *284*(5), 2719.
[27] S. Luo, D. C. Rubinsztein, *Autophagy* **2013**, *9*(1), 104.
[28] K. Liu, J. Huang, M. Xie, Y. Yu, S. Zhu, R. Kang, L. Cao, D. Tang, X. Duan, *Autophagy* **2014**, *10*(3), 442.
[29] I. Sirois, J. Groleau, N. Pallet, N. Brassard, K. Hamelin, I. Londono, A. V. Pshezhetsky, M. Bendayan, M. J. Hébert, *Autophagy* **2012**, *8*(6), 927.
[30] R. Núñez, S. M. Sancho-Martínez, J. M. L. Novoa, F. J. López-Hernández, *Cell Death Differ.* **2010**, *17*(11), 1665.
[31] H. Wu, X. Che, Q. Zheng, A. Wu, K. Pan, A. Shao, Q. Wu, J. Zhang, Y. Hong, *Int. J. Biol. Sci.* **2014**, *10*(9), 1072.
[32] L. A. Booth, S. Tavallai, H. A. Hamed, N. Cruickshanks, P. Dent, *Cellular Signalling* **2014**, *26*(3), 549.

SUPPORTING INFORMATION

Additional supporting information can be found online in the Supporting Information section at the end of this article.

How to cite this article: L. Zhao, H. Wang, S. Liu, T. Xi, L. Wang, Y. Li, L. Chen, R. Jianping, K. X. Liang, *J. Biochem. Mol. Toxicol.* **2022**, e23280.
https://doi.org/10.1002/jbt.23280